



**POLITECNICO**  
MILANO 1863

[RE.PUBLIC@POLIMI](mailto:RE.PUBLIC@POLIMI)

Research Publications at Politecnico di Milano

## Post-Print

This is the accepted version of:

A. Guardone, P. Colonna, E. Casati, E. Rinaldi  
*Non-Classical Gas Dynamics of Vapour Mixtures*  
Journal of Fluid Mechanics, Vol. 741, 2014, p. 681-701  
doi:10.1017/jfm.2013.13

The final publication is available at <https://doi.org/10.1017/jfm.2013.13>

Access to the published version may require subscription.

This article has been published in a revised form in Journal of Fluid Mechanics [<https://doi.org/10.1017/jfm.2013.13>]. This version is free to view and download for private research and study only. Not for re-distribution, re-sale or use in derivative works. © 2014 Cambridge University Press

**When citing this work, cite the original published paper.**

Permanent link to this version

<http://hdl.handle.net/11311/861148>

# Nonclassical gasdynamics of vapour mixtures

By ALBERTO GUARDONE<sup>1</sup>, PIERO COLONNA<sup>2</sup>,  
EMILIANO CASATI<sup>2,3</sup> AND ENRICO RINALDI<sup>2</sup>

<sup>1</sup>Department of Aerospace Science and Technology, Politecnico di Milano  
Via La Masa 34, Milano, 20156, Italy

<sup>2</sup>Propulsion & Power, Delft University of Technology  
Kluyverweg 1, Delft, 2629 HS, The Netherlands

<sup>3</sup>Energy Department, Politecnico di Milano  
Via Lambruschini 4, Milano, 20156, Italy

(Received 5 December 2013)

The nonclassical gasdynamics of binary mixtures of organic fluids in the vapour phase is investigated for the first time. A predictive thermodynamic model is used to compute the relevant mixture properties, including its critical point coordinates and the local value of the fundamental derivative of gasdynamics  $\Gamma$ . The considered model is the improved Peng-Robinson Stryjek-Vera cubic equation of state, complemented by the Wong-Sandler mixing rules. A finite thermodynamic region is found where the non-linearity parameter  $\Gamma$  is negative and therefore nonclassical gasdynamics phenomena are admissible. A non monotone dependence of  $\Gamma$  on the mixture composition is observed in the case of binary mixtures of siloxane and perfluorocarbon fluids, with the minimum value of  $\Gamma$  in the mixture being always larger than that of its more complex component. The observed dependence indicates that non-ideal mixing has a strong influence on the gasdynamics behaviour—either classical or nonclassical—of the mixture. Numerical experiments of the supersonic expansion of a mixture flow around a sharp corner shows the transition from the classical configuration, exhibiting an isentropic rarefaction fan centred at the expansion corner, to nonclassical ones, including mixed expansion waves and rarefaction shock waves, if the mixture composition is changed.

---

## 1. Introduction

The first scientist who hinted at the possibility of observing rarefaction shock waves in vapours of molecularly complex organic fluids was Nobel-laureate Hans [Bethe \(1942\)](#). Rarefaction shock waves are discontinuous solutions to the Euler equations of compressible flows where the fluid undergoes an irreversible expansion process which results into a discontinuous reduction of density, pressure, temperature and fluid velocity in the direction of propagation of the shock wave. As it is well known, rarefaction shock waves are not physically admissible in dilute gases with constant specific heats.

In a broad theoretical study on the theory of shock waves in any material, Bethe outlined how the occurrence of rarefaction shock waves depends on a peculiar combination of the thermodynamic properties of the material at the states of interest. He noticed that according to the [van der Waals \(1988\)](#) model, rarefaction shock waves would theoretically be possible in the dense vapour of fluids featuring high values of the heat capacity, if the pre- and post-shock states of the fluid are close to the vapour-liquid critical point. Nevertheless, he ruled out this possibility on the ground of what we now

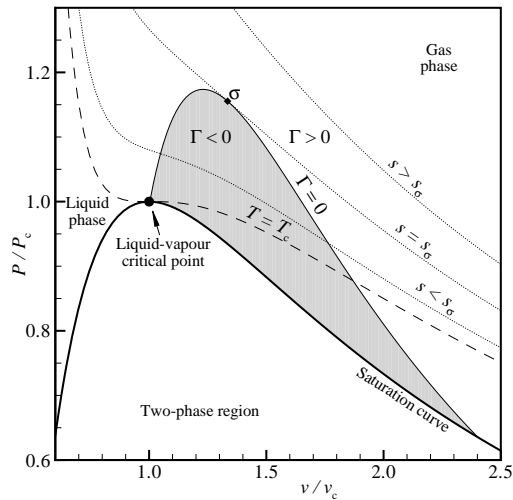


Figure 1: From [Guardone \*et al.\* \(2010\)](#). Liquid-vapour saturation curve (—) and  $\Gamma < 0$  region (shaded region) for a BZT fluid in the volume-pressure plane computed from van der Waals model under the assumption of a constant isochoric specific heat  $c_v$  and for  $c_v/R = 2000$ , with  $R$  gas constant. Selected isentropes ( $\cdots$ ) and the critical isotherm  $T = T_c$  (—) are also indicated. Note that the isentropes are concave down in the  $\Gamma < 0$  region. The isentrope  $s_\sigma$  is tangent to the  $\Gamma = 0$  line in  $\sigma$ .

know as incorrect physical arguments, see also [Thompson & Lambrakis \(1973\)](#). An early contribution is also due to [Zel'dovich \(1946\)](#) and [Weyl \(1949\)](#). Though, it was [Thompson \(1971\)](#), see also [Thompson & Lambrakis \(1973\)](#); [Thompson \(1988\)](#), who first provided a systematic treatment of what is now called non classical gas dynamics. A review article by [Kutateladze \*et al.\* \(1987\)](#) documents the advancements in non classical gasdynamics until the 80's, while a more recent review can be found in [Kluwick \(2001\)](#).

A necessary condition for non classical behaviour to be physically admissible is that the fundamental derivative of gas dynamics

$$\Gamma \equiv 1 + \frac{\rho}{c} \left( \frac{\partial c}{\partial \rho} \right)_s = \frac{v^3}{2c^2} \left( \frac{\partial^2 P}{\partial v^2} \right)_s, \quad (1.1)$$

a thermodynamic property of the fluid first introduced by [Hayes \(1960\)](#), is negative. In definition (1.1),  $\rho$  is the density,  $s$  is the entropy,  $P$  is the pressure,  $v = 1/\rho$  is the specific volume, and  $c$  is the zero-frequency speed of sound  $c \equiv (\partial P / \partial \rho)_s$ . If  $\Gamma$  is negative in a finite thermodynamic region, rarefaction shocks are possible, among other so-called non classical waves such as composite and split waves, see, e.g. [Thompson \(1971\)](#).

Substances characterized by thermodynamic states featuring negative values of  $\Gamma$  in the dense vapour phase are called Bethe-Zel'dovich-Thompson (BZT) fluids. The region of negative  $\Gamma$  in the vapour phase is shown in figure 1 in the pressure-specific volume thermodynamic diagram of a paradigmatic BZT fluid, where the  $\Gamma = 0$  line and the vapour saturation line delimit the negative- $\Gamma$  region. The studies of Thompson sparked quite some interest in the following years, and many investigations expanded the theory covering several nonclassical phenomena and aspects, see, e.g., [Cramer & Kluwick \(1984\)](#); [Cramer & Sen \(1986, 1987\)](#); [Menikoff & Plohr \(1989\)](#); [Cramer \(1989\)](#); [Cramer & Sen \(1990\)](#); [Cramer & Crickenberger \(1991\)](#); [Cramer \(1991\)](#); [Kluwick & Meyer \(2010\)](#). One

of the latest developments is related to the investigation of nonclassical phenomena in the vapour-liquid critical point region of any common fluid, see [Nannan \*et al.\* \(2013\)](#).

Experimental evidence of nonclassical gasdynamics is available only for two-phase vapor-liquid, see [Thompson \*et al.\* \(1986\)](#); [Gulen \*et al.\* \(1989\)](#); [Thompson \(1991\)](#), or solid-solid, see [Ivanov & Novikov \(1961\)](#), systems. In the single-phase vapour region, only classical gasdynamics phenomena have been observed so far. Notably, in the former Soviet Union, [Borisov \*et al.\* \(1983\)](#) made an attempt to experimentally prove the existence of a rarefaction shock wave (RSW), using a special shock tube. The interpretation of the results of the experiments, arguably a rarefaction shock front developing in the tube, has later been confuted in the light of additional knowledge and simulation capability ([Ferguson 2001](#); [Kluwick 2001](#); [Nannan \*et al.\* 2013](#)). Theoretical studies ([Chandrasekar & Prasad 1991](#); [Cramer \*et al.\* 1992](#); [Schnerr & Molokov 1994, 1995](#); [Aldo & Argrow 1995](#); [Brown & Argrow 1998](#)), and new simulation capabilities ([Schnerr & Leidner 1993a,b](#); [Argrow 1996](#); [Monaco \*et al.\* 1997](#); [Brown & Argrow 1997, 2000](#); [Cinnella & Congedo 2007, 2008](#); [Cinnella 2008](#)), paved the way to a new experimental attempt in 2000 at the University of Boulder ([Ferguson 2001](#); [Ferguson \*et al.\* 2001, 2003](#)). The failed experiment put into evidence one of the major obstacles, namely that the BZT thermodynamic region (the region comprising the states featuring negative- $\Gamma$ , see figure 1) is very close to the thermal decomposition temperature of suitable organic fluids, which is in the range 350–400 °C. In addition, the repeatable rupture of the shock-tube diaphragm proved unattainable due to the small pressure difference ([Thompson & Loutrel 1973](#); [Guardone 2007](#); [Colonna \*et al.\* 2008a](#)).

Much attention has recently been devoted to the identification of BZT fluids, and to the computation of the negative- $\Gamma$  region, see [Colonna \*et al.\* \(2009\)](#) for a review. More recently [Colonna \*et al.\* \(2008a\)](#) started a new project aimed at the generation and measurement of a rarefaction shock wave in a newly conceived Ludwig-tube-type setup. A siloxane fluid, D<sub>6</sub>, has initially been selected as the working fluid. Siloxanes are especially suited for the RSW experiment because of available knowledge on their thermal stability ([Angelino & Invernizzi 1993](#); [Colonna 1996](#)), thermodynamic properties ([Colonna \*et al.\* 2006](#); [Nannan \*et al.\* 2007](#); [Colonna \*et al.\* 2008b](#); [Nannan & Colonna 2009](#))), and their use as working fluids in thermal energy conversion systems, see, e.g., [Angelino & Colonna \(1998\)](#); [Uusitalo \*et al.\* \(2013\)](#); [Lang \*et al.\* \(2013\)](#). Few of the compounds of the siloxane family are candidate BZT fluids ([Colonna \*et al.\* 2007](#)).

The design of the rarefaction shock wave experiment drove studies aimed at better identifying the thermodynamic region within which nonclassical phenomena are admissible ([Zamfirescu \*et al.\* 2008](#)), and the maximum pressure difference and shock wave Mach number that can be expected ([Guardone \*et al.\* 2010](#)). Given that the experimental conditions are difficult to realize and that the rarefaction shock wave is expected to be weak, therefore more challenging to measure, uncertainty quantification applied to flow simulations has been preliminarily used as an aid in determining the optimal experimental conditions ([Congedo \*et al.\* 2012](#)).

The present work is motivated by several observations about mixtures of organic fluids. Differently from mixtures of ideal gases, thermodynamic properties of dense vapours of multicomponent mixtures do not scale linearly with the mole fractions of each compound, as molecular interaction among different molecules plays a major role. Typical examples of non-ideal behaviour of fluids mixtures are the critical temperature, pressure and specific volume of a binary mixture, which usually differ from that of each of the constituents. The same holds for the melting point and for most thermodynamic properties. The fundamental derivative of gasdynamics  $\Gamma$ , being a derived thermodynamic property, is also affected by non-ideal mixing effects, as preliminarily discussed

in Colonna & Silva (2003a). In addition, experiments on the thermal stability of siloxane mixtures (Angelino & Invernizzi 1993; Colonna 1996), and a deeper understanding on the chemistry of thermal decomposition of poly-dimethyl siloxanes (Dvornic 2004), show that, at temperatures close to the so-called temperature stability limit, a pure siloxane undergoes a transformation called *rearrangement*, whereby small quantities of other compounds of the same family are formed. Such mixture composition is then thermally stable at that temperature over time. The composition of the mixture is therefore a new relevant variable in the study of BZT fluids, and, importantly, mixtures of organic fluids are also considered for applications in organic Rankine cycle (ORC) power systems (Angelino & Colonna 1998, 2000; Chen *et al.* 2011; Trapp & Colonna 2013), one of the possible applications of nonclassical gasdynamics (Brown & Argrow 2000).

In the present preliminary study on mixtures as BZT fluids, siloxanes and perfluorocarbons have been considered as constituents. Suitable thermodynamic models for multi-component fluids are briefly discussed in §2. Their limitation in terms of accuracy of the predicted  $\Gamma$  values is also addressed. These models are used to estimate the boundaries of the thermodynamic region of admissibility of rarefaction shock waves, and the influence of the mixture composition. In §3, exemplary simulation of a supersonic flow expanding over a wedge, whereby the composition of the mixture is varied, are presented to assess the influence of the molecular composition on the gasdynamics behaviour. Concluding remarks and an outlook on future research are given in §4.

## 2. Admissibility region for rarefaction shock waves in dense gas mixtures

Modelling non-ideal thermodynamic properties of fluid mixtures—including the determination of the fundamental derivative of gasdynamics  $\Gamma$ —requires to correctly account for the interaction between different molecules, an added degree of difficulty with respect to pure-fluid thermodynamics. No fundamental and general theory on the interaction of different molecules exists yet, therefore no accurate model is available. For these reasons the estimation of mixture properties is affected in general by larger uncertainties, if compared to the estimation of pure-fluid properties. Mixtures of simple molecules, e.g., light gases and simple hydrocarbons, can be modelled with relatively high accuracy, and reference equations of state have been developed (Kunz *et al.* 2007). These semi-empirical models rely on large sets of accurate fluid property measurements. Unfortunately, accurate property measurements of complex organic compounds are not available. In order to estimate dense-vapour thermodynamic properties of mixtures of complex organic fluids, simpler so-called predictive equations of state must be adopted, see, e.g., Sandler (1989, 1993). These models rely on a small set of data related to the pure constituents, and to parameters describing the interaction between different molecules; these parameters can be determined either experimentally or estimated. Predictive models applicable to mixtures are thermodynamically consistent, but calculated property values are affected by much larger uncertainties if compared to the estimation of pure-fluid properties.

In this study the properties of mixtures of siloxanes and perfluorocarbons are evaluated with either the improved Peng-Robinson Stryjek-Vera cubic equation of state (van der Stelt *et al.* 2012), complemented by the Wong-Sandler mixing rules (iPRSV-WS), see (Wong & Sandler 1992a; Coutsikos *et al.* 1995b), or the PC-SAFT model (Gross & Sadowski 2001), which is formulated in terms of molecular parameters whose value depends on the molecular arrangement. Since most of the treatment in this paper is based on the use of the iPRSV-WS model, both the functional form of the equation of state and the derivation of the adopted mixing-rules are recalled in Appendix A. These models, together with

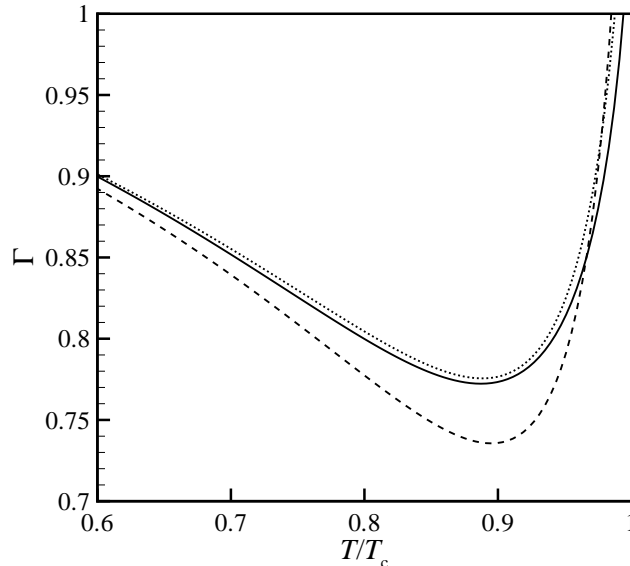


Figure 2: Comparison of  $\Gamma$  values along the dew line as a function of the reduced temperature  $T/T_c$  for the equimolar mixture of propane and pentane calculated with the reference model by [Kunz \*et al.\* \(2007\)](#) (—), the iPRSV-WS ( $\cdots$ ), and PC-SAFT (— — —) thermodynamic models.

others, are implemented in an in-house computer library for the calculation of primary and secondary thermodynamic properties of fluids ([Colonna \*et al.\* 2012](#)).

Information on how the data for the iPRSV-WS model applied to siloxane mixtures were obtained can be found in [Angelino & Colonna \(1998\)](#). The analytical expression of  $\Gamma$  for this thermodynamic model is reported in [Colonna & Silva \(2003a\)](#). The application of the PC-SAFT model to linear siloxanes is documented in [Lai \*et al.\* \(2009\)](#), and has been extended by the authors to model also cyclic siloxanes. Siloxane/perfluorocarbon mixtures are modelled with the iPRSV-WS equation of state starting from experimental values of the critical point of these mixtures ([Armenio 2009](#)), and compared to results from the PC-SAFT model. Such a comparison is the only possible assessment at the moment, since no other experimental values are available. Values of  $\Gamma$  for the PC-SAFT mixture model are calculated with analytical expressions obtained by derivation from the equation of state and the isobaric ideal-gas heat capacity relation, see for example [Colonna \*et al.\* \(2009\)](#) and [Nannan \*et al.\* \(2013\)](#).

Figure 2 shows a comparison between the values of  $\Gamma$  calculated along the dew line for the equimolar mixture of propane and pentane using a reference model ([Kunz \*et al.\* 2007](#)), the iPRSV-WS and the PC-SAFT models. As it is known, see [Abbott \(1973\)](#); [Bymaster \*et al.\* \(2008\)](#), predictive models fail to accurately estimate properties close to the vapour-liquid critical point, therefore also  $\Gamma$  values at high reduced temperature  $\tilde{T} = T/T_c$  deviate from those obtained with the reference model, cf. figure 2. A number of evaluations for various fluids modelled by the reference model of [Kunz \*et al.\* \(2007\)](#) revealed that the iPRSV-WS model performs better than the PC-SAFT model in the critical-point region, therefore it has been chosen for the analysis presented in §3.

Figure 3 shows the negative- $\Gamma$  region (also termed BZT region) in the  $P$ - $T$  thermo-

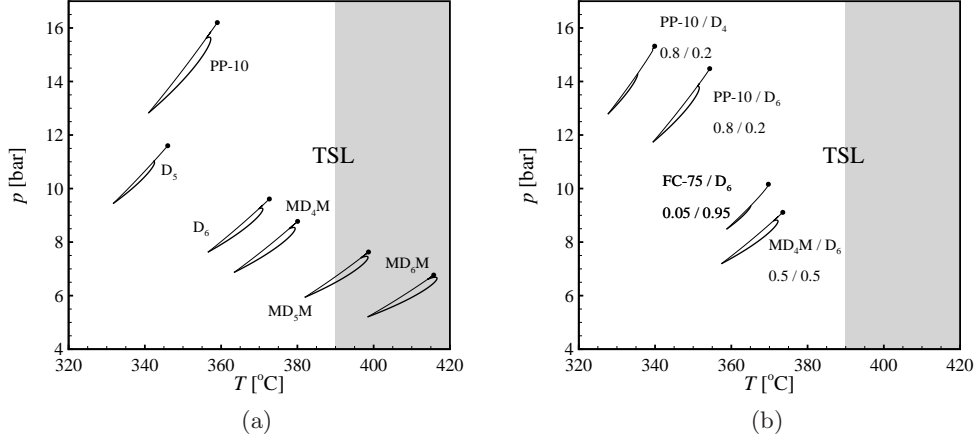


Figure 3: Negative  $\Gamma$  region (or BZT region) in the  $P$ - $T$  thermodynamic plane for several pure fluids (3a) and some selected mixtures (3b): values are calculated with the iPRSV-WS thermodynamic model. For each fluid, the circle indicate the critical point. It is relevant to future experiments on non-classical gasdynamic phenomena that the temperature values are close to the estimated thermal stability limit (TSL) for these organic compounds in contact with stainless steel ( $\approx 390^\circ\text{C}$ ), while the values of pressure are comparatively moderate. The shaded area indicates the range of temperatures where thermal decomposition in stainless steel can be expected.

Table 1: Molar fraction  $x$ , average molecular weight MW, critical pressure  $P_c$ , critical temperature  $T_c$ , critical density  $\rho_c$  and minimum value of the fundamental derivative of gasdynamics  $\Gamma_{\min}$  for a mixture of siloxane fluids MDM and MD<sub>6</sub>M.

$x$		MW	$P_c$	$T_c$	$\rho_c$	$\Gamma_{\min}$
MDM	MD <sub>6</sub> M	[g/mole]	[bar]	[K]	[kg/m <sup>3</sup> ]	[-]
1.00	0.00	236.5	14.2	564.1	229.38	0.0917
0.75	0.25	329.2	18.0	653.9	288.41	0.5676
0.40	0.60	459.0	11.7	687.5	260.34	0.2567
0.15	0.85	551.7	8.3	690.3	243.09	-0.1187
0.05	0.95	588.8	7.2	689.6	236.65	-0.3040
0.00	1.00	607.3	6.8	689.0	230.64	-0.4001

dynamic plane for several selected organic compounds of the family of siloxanes, fluorocarbons, perfluorocarbons and their mixtures, calculated with the iPRSV-WS model. The ensemble of fluid thermodynamic states featuring a negative value of  $\Gamma$  in the dense vapour phase is delimited by the dew line on the left and by the concave-upward  $\Gamma = 0$  line on the right. An estimate of the temperature at which thermal break-down in stainless steel is likely to occur is also indicated (TSL, Thermal Stability Limit).

As an example, in table 1, the molar fraction  $x$ , average molecular weight MW, critical pressure  $P_c$ , critical temperature  $T_c$ , critical density  $\rho_c$  and minimum value of the fundamental derivative of gasdynamics  $\Gamma_{\min}$  for the mixture of siloxane fluids MDM and

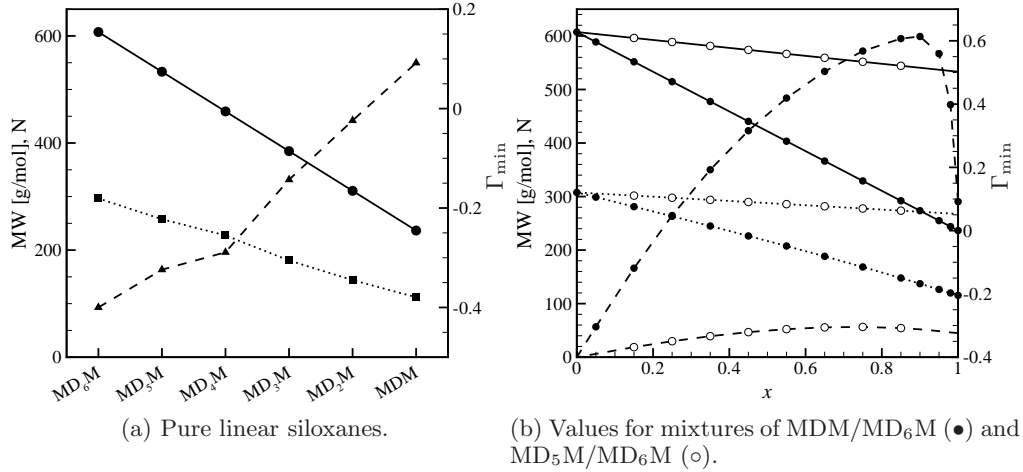


Figure 4: Molecular weight MW (—), active degrees of freedom evaluated at the critical temperature  $N$  (···) and minimum value of  $\Gamma$  along the dew line (---) for selected linear siloxanes. Properties are calculated with the iPRSV equation of state for the pure fluids, see [van der Stelt \*et al.\* \(2012\)](#), while the equation of state is complemented by the Wong–Sandler mixing rules [Wong & Sandler \(1992b\)](#) for the mixtures.

MD<sub>6</sub>M are reported. Thermodynamic properties are calculated using the iPRSV-WS thermodynamic model. As it is well known, the critical point coordinates in table 1 depend in a non-linear fashion on the mixture composition  $x$ , with the critical pressure, temperature and density exhibiting a local maximum.

Admittedly, the negative- $\Gamma$  region of fluids MD<sub>5</sub>M and MD<sub>6</sub>M is partially or completely past the TSL, see figure 3. Although mixtures are expected to be more thermally stable than their pure components, such high values of operating temperatures are unrealistic, if stainless steel is the containing material. Moreover, for MD<sub>5</sub>M and MD<sub>6</sub>M the negative- $\Gamma$  region is very close to the liquid-vapour saturation point, where the value of  $\Gamma$  is expected to diverge to infinity [Nannan \*et al.\* \(2013\)](#). In this region, an accurate evaluation of the thermodynamic properties, including  $\Gamma$ , would require the inclusion of a critical point scaling law and of a cross-over model linking the latter with the analytical EoS. In the present qualitative study fluid MD<sub>6</sub>M was considered in order to maximize the strength of non-classical phenomena for illustration purposes; thermal decomposition and critical point effects are to be carefully assessed before selecting this fluid for the experiments. However, it is remarkable that, similarly to previous studies on non-classical gasdynamics, the present findings are directly applicable to less complex molecules, because the qualitative fluid dynamic behaviour is similar to that of MD<sub>6</sub>M.

Results shown in figure 4 are a preliminary evaluation of the dependence of the minimum value of  $\Gamma$  on the molecular weight and on the molecular complexity, which is defined here as the equivalent number of active translational, rotational and vibrational degrees of freedom of the molecules at the critical temperature and in the dilute gas limit, see [Colonna & Guardone \(2006\)](#). The molar composition is also indicated for mixtures. As it is known, in the case of pure fluids the minimum value of  $\Gamma$  along the dew line,  $\Gamma_{\min}$ , decreases monotonically with increasing molecular weight and complexity (figure 4a). In



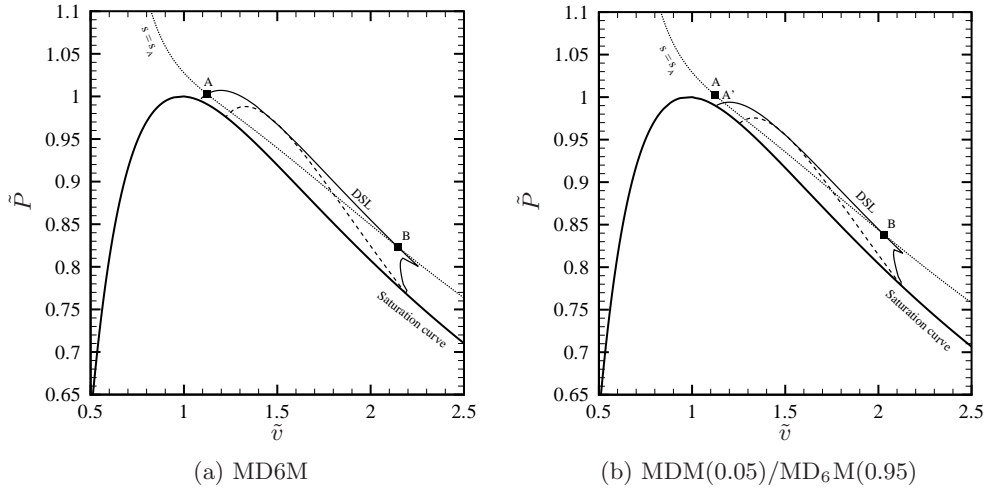


Figure 5: Pre- (A) and post-expansion (B) states on the reduced  $P$ - $v$  plane. The negative- $\Gamma$  region (dashed line) and DSL are also reported.

addition, the extension of the BZT region in the  $P$ - $T$  plane increases with increasing molecular weight and complexity, cf. figure 3a.

It is remarkable that the effect of mixing, therefore of intermolecular interaction, alters the non monotone dependency of  $\Gamma_{\min}$  from molecular weight and complexity. Figure 4b shows that for binary mixtures of the siloxane fluids MDM/MD<sub>6</sub>M and MD<sub>5</sub>M/MD<sub>6</sub>M the estimated value of  $\Gamma_{\min}$  does not decrease monotonically with increasing average molecular complexity and weight of the mixture, similarly to what observed for the values of the critical pressure, temperature and density in table 1. Indeed, for both the MDM/MD<sub>6</sub>M and the MD<sub>5</sub>M/MD<sub>6</sub>M mixtures, the value of  $\Gamma_{\min}$  exhibits a maximum value, which is at  $x_{\text{MDM}} \approx 0.75$  for MDM/MD<sub>6</sub>M, and at  $x_{\text{MD}_5\text{M}} \approx 0.9$  for MD<sub>5</sub>M/MD<sub>6</sub>M, with  $x$  the mole fraction. Notably, for the mixture MDM(0.4)/MD<sub>6</sub>M(0.6) the value of  $\Gamma_{\min}$  is largely different, even in sign, from the one predicted for MD<sub>4</sub>M, which is the homologous pure fluid in terms of molecular weight and complexity. This type of dependency of  $\Gamma_{\min}$  on molar composition is predicted also in case of mixtures of alkanes, by using reference equations of state for the calculation of thermodynamic properties.

In the case presented here, the variation of  $\Gamma_{\min}$  with the mole fraction of a binary mixture is such that, for any given composition,  $\Gamma_{\min}$  is always larger than the molar-fraction averaged value of  $\Gamma_{\min}$  of the two pure constituents. Due to the large variety of intermolecular forces, it cannot currently be ruled out that an opposite trend can be observed, namely that the mixing of two or more fluids leads to values of  $\Gamma_{\min}$  that are lower than those of the mixture constituents.

From the knowledge of the fundamental derivative of gasdynamics in the vapour phase, the thermodynamic conditions resulting in nonclassical gasdynamics waves can be determined. The conditions for the admissibility of rarefaction shocks are given by Zamfirescu *et al.* (2008), where the method for determining the so called *rarefaction shock region* (RSR) is also reported.

In figure 5a the RSR of siloxane fluid MD<sub>6</sub>M is shown, together with a representative

isentrope  $s = s_A$ . As detailed in [Zamfirescu \*et al.\* \(2008\)](#), the RSR is the thermodynamic region that includes all the states that can possibly be upstream and downstream of a rarefaction shock wave. By definition, the RSR embeds the negative- $\Gamma$  region. For pure fluids, the size of the RSR increases with molecular complexity, similarly to the BZT region. In particular, the RSR is limited by the vapour-liquid saturation (VLE) curve and by the Double Sonic Line (DSL), which is the locus of all fluid states that can be connected by a double-sonic shock, whereby the pre- and post-shock states are sonic. The DSL and the VLE are connected by the two loci representing the upstream state of upstream-sonic downstream-saturated rarefaction shocks and the downstream state of upstream-saturated downstream-sonic rarefaction shock wave.

Each isentrope intersects the DSL in two points A and B, with  $v_A < v_B$ . At point A the Rayleigh line connecting point A and B is tangent to both the isentrope trough A and the shock adiabat trough A. At point B, it is tangent to the isentrope trough B and the shock adiabat trough A. Therefore, the shock connecting point A and B is a double sonic shock, with sonic state in both point A and B. The RSW connecting point A and B encompasses the largest possible pressure difference, i.e., is the strongest possible RSW originating from the considered isentrope. Note that in [figure 5a](#) the shock adiabat through A and the isentrope  $s = s_A$  are not distinguishable.

The RSR of mixtures is calculated with the same procedure as for pure fluids, with no modifications. An example is given in [figure 5b](#), where the RSR for the mixture MDM(0.05)/MD<sub>6</sub>M(0.95) is shown. The increase of the MDM percentage in the mixture MDM/MD<sub>6</sub>M causes the rarefaction shock region to reduce its size in the  $v$ - $P$  plane, if compared to the one of pure MD<sub>6</sub>M.

### 3. Nonclassical gasdynamics behaviour of dense gas mixtures

A preliminary study on the effect of the mixture composition on the gasdynamic behaviour of mixtures of organic fluids has been carried out. To this purpose, the supersonic expansion of the dense vapour of a mixture over a corner is simulated.

The selected mixture is composed by MD<sub>6</sub>M, a BZT fluid, and MDM, a fluid for which no suitable thermodynamic model predicts a negative- $\Gamma$  region. To compare results for different mixture composition, a common upstream state was selected in terms of dimensionless quantities. The upstream state features the same value of the Mach number  $M$ , reduced pressure  $\tilde{P} \equiv P/P_c$ , and non-dimensional entropy  $\tilde{s} = s/s_\tau$  for all simulations. The locus  $s = s_\tau$  is the isentrope tangent to the saturation line. The choice of  $\tilde{P}$  and  $\tilde{s}$  to identify the upstream flow state is motivated by the fact that they identify homologous thermodynamic states in the  $P$ - $v$  thermodynamic plane, with comparable real gas effects.

The values of  $M$ ,  $\tilde{P}$  and  $\tilde{s}$  identifying the upstream states for the simulations are reported in [table 2](#). The solid surface past the corner forms an angle of  $-13.169^\circ$  with respect to the free-stream direction. These values have been chosen so that in the case of pure MD<sub>6</sub>M a rarefaction shock wave with maximum intensity is obtained, which forms an angle of  $60^\circ$  with respect to the free-stream direction, see [Guardone \*et al.\* \(2010\)](#).

The computer program used to perform the simulations is a parallel solver for the Navier-Stokes equations on unstructured meshes based on a finite volume formulation and implicit time-integration ([Pecnik \*et al.\* 2012b](#)). The code has been recently extended to include real gas properties ([Pecnik \*et al.\* 2012a](#)) using a general interface to several thermodynamic libraries ([Colonna \*et al.\* 2012](#)). An unstructured mesh refinement technique is adopted to increase the accuracy in regions where the solutions exhibit the largest gradients.

[Figure 6](#) shows the flow field isobars from flow simulations for different mixtures of

Table 2: Upstream states for the simulations of the supersonic flow of a dense gas mixture over an expansion corner.

$M_A$	$\tilde{s}_A$	$\tilde{P}_A$
1.15470	1.00276	1.00217

Table 3: Upstream and downstream thermodynamic states for the different mixtures considered in the simulations.

Composition $x$		Upstream state A				Downstream state B				
MDM	MD <sub>6</sub> M	$\tilde{T}_A$	$\tilde{\rho}_A$	$\Gamma_A$	$Z_A$	$\tilde{P}_B$	$\tilde{T}_B$	$\tilde{\rho}_B$	$\Gamma_B$	$Z_B$
1.00	0.00	1.0008	0.8630	1.0823	0.3610	0.8461	0.9833	0.5279	0.2078	0.5072
0.75	0.25	1.0133	0.8280	1.1866	0.4510	0.7764	1.0013	0.5172	0.5912	0.5661
0.40	0.60	1.0027	0.9234	1.0741	0.3912	0.8284	0.9931	0.5698	0.3292	0.5291
0.15	0.85	1.0012	0.9059	0.9290	0.3617	0.8485	0.9919	0.5342	0.1593	0.5241
0.05	0.95	1.0008	0.8785	0.8148	0.3577	0.8382	0.9910	0.4920	0.1664	0.5395
0.00	1.00	1.0005	0.8824	0.7310	0.3532	0.8231	0.9902	0.4660	0.2068	0.5551

Table 4: Downstream Mach number and pressure, temperature, density, and velocity differences across the expansion waves, where  $\Delta(\cdot) = (\cdot)_B - (\cdot)_A$ .

Composition $x$		$M_B$	$\frac{\Delta P}{P_A}$	$\frac{\Delta T}{T_A}$	$\frac{\Delta \rho}{\rho_A}$	$\frac{\Delta u}{u_A}$
MDM	MD <sub>6</sub> M					
1.00	0.00	1.1770	-0.1562	-0.0175	-0.3927	0.4128
0.75	0.25	1.3822	-0.2257	-0.0119	-0.3760	0.3222
0.40	0.60	1.2426	-0.1739	-0.0096	-0.3843	0.3752
0.15	0.85	1.1109	-0.1539	-0.0093	-0.4140	0.4943
0.05	0.95	1.0621	-0.1641	-0.0098	-0.4483	0.6195
0.00	1.00	1.0450	-0.1792	-0.0103	-0.4765	0.7283

MDM/MD<sub>6</sub>M, whereby the mole fraction of MDM varies from  $x_{\text{MDM}} = 1$  in figure 6a to  $x_{\text{MDM}} = 0$  in figure 6f, under the assumption of negligible fluid viscosity and thermal conductivity.

Figure 6a displays the supersonic flow of a pure MDM vapour. As expected, since  $\Gamma > 0$ , a classical isentropic expansion fan is observed in this case. It is remarkable that differently from supersonic expansions of a constant specific heats ideal gas, the Mach number  $M$  variation across the expansion is non-monotone, as it can be appreciated from figure 7a, where the Mach number is depicted for a representative streamline across the expansion wave. The present non monotone behaviour is consistent with the value of the parameter  $J$ , namely,

$$J(s, \rho, M) = 1 - \Gamma(s, \rho) - \frac{1}{M^2}. \quad (3.1)$$

across the expansion wave. Indeed, for isentropic processes from a given state A one has,

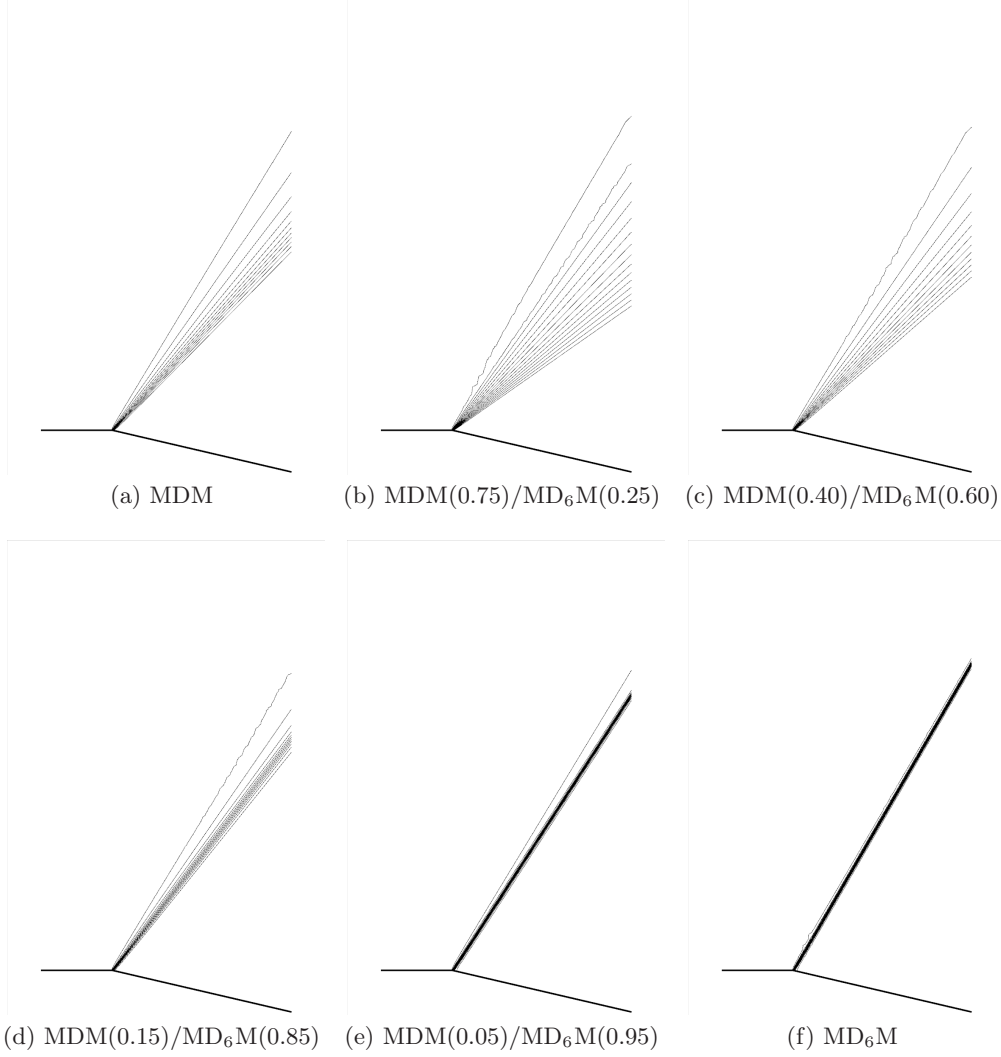
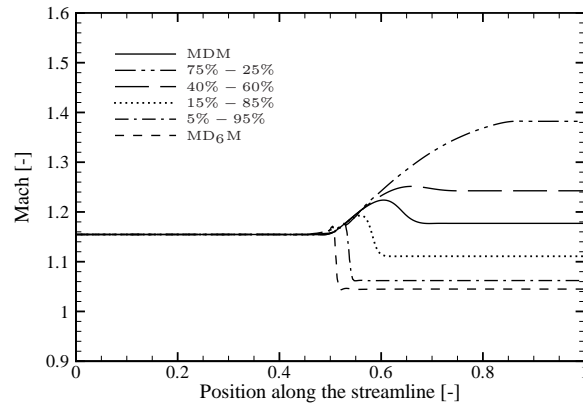


Figure 6: Simulated flows of dense vapours of MDM/MD<sub>6</sub>M expanding over a corner, whereby the mole fraction of MDM varies from 1 (a) to 0 (f). Fifteen levels of isopressure contour lines are plotted in the range  $\tilde{P} = [0.8, 1]$ . The upstream state features the same Mach number  $M$ , reduced pressure  $\tilde{P} \equiv P/P_c$  and reduced entropy  $\tilde{s} = s/s_\tau$  in all cases. The fluid thermodynamic model is the iPRSV equation of state complemented by the Wong-Sandler mixing rules for the mixtures.

see [Cramer & Best \(1991\)](#),

$$\frac{dM}{d\rho} = J(s_A, \rho, M) \frac{M}{\rho}. \quad (3.2)$$

As shown in figure 7b, in the expansion of pure MDM vapour depicted in figure 6a,  $J$  assumes both negative and positive values and therefore  $M$  is non-monotone. Note that for a constant specific heat ideal gas,  $J = (1 - \gamma)/2 - 1/M^2 < 0$ , with  $\gamma$  ratio of the isobaric and isochoric specific heats, and therefore  $M$  always increase monotonically during a supersonic expansion.



(a) Mach number

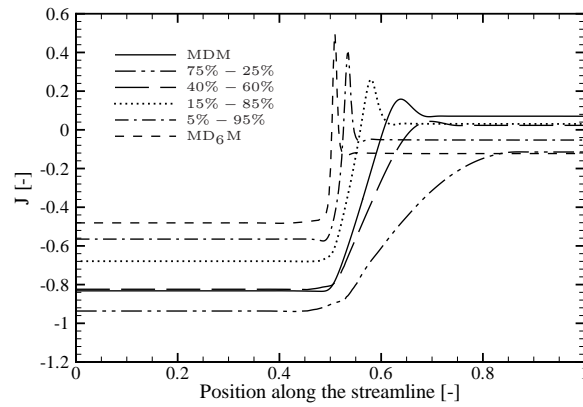
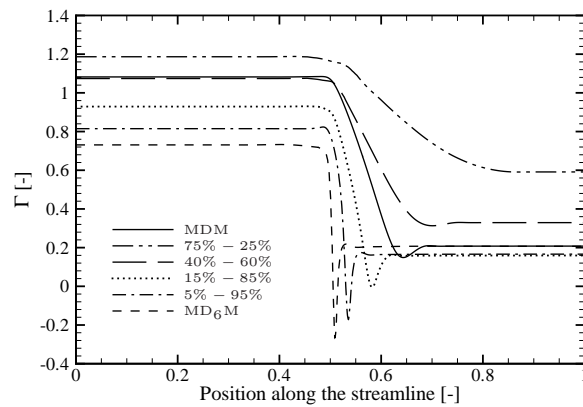
(b)  $J = 1 - \Gamma - 1/M^2$ (c)  $\Gamma$ 

Figure 7: Variation of the Mach number (top), the parameter  $J = 1 - \Gamma - 1/M^2$  (middle), and  $\Gamma$  (bottom) along a streamline. Different lines correspond to different compositions of the mixture MDM/MD<sub>6</sub>M.

A reversed, nonclassical, behaviour is observed for the supersonic expansion of pure MD<sub>6</sub>M, shown in figure 6f. An oblique nonclassical rarefaction shock wave, which forms an angle of 60° with respect to the upstream flow direction, is observed.

Intermediate situations are observed in the case of mixtures of MDM/MD<sub>6</sub>M—shown in figures 6b, 6c, 6d and 6e—where the supersonic expansions of mixtures of increasing concentration of the more complex component MD<sub>6</sub>M are depicted.

In particular, in figure 6b, where the flow of a MDM(0.75)/MD<sub>6</sub>M(0.25) mixture is shown, a classical rarefaction fan is observed since  $\Gamma > 0$  in the vapour phase. The angular sector encompassed by the fan is larger than that observed in figure 6a for pure fluid MDM, although the final turning angle  $\theta_B = -13.169^\circ$  is the same in both conditions. Therefore, since the slope of the limiting characteristic line at the right boundary of the fan is  $\lambda(\theta_B) = \tan(\theta_B + \mu(\theta_B))$  where  $\sin \mu_B = 1/M_B$ , one can conclude that the Mach number at the end of the expansion is larger in this case, as it is confirmed also by the values in table 3 and 4. The above can be explained by recalling the dependence of the Mach number on the local velocity angle  $\theta$  given by the Prandtl-Meyer relation, see Thompson (1988), namely,

$$d\theta = \frac{\sqrt{M^2 - 1}}{1 - (\Gamma - 1)M^2} dM. \quad (3.3)$$

Indeed, despite the larger average molecular weight, along the considered isentrope the value of  $J$  for the mixture is always lower than that computed for pure MDM, see figure 7b, and the Mach number difference between the upstream and downstream state is larger.

In the conditions depicted in 6c and 6d,  $\Gamma_{\min} > 0$ , see figure 3 and table 1, and therefore a classical flow is observed in both cases. In case 6c, the Mach number in state B is larger than that observed in case 6a, consistently with  $\Gamma$  and  $J$  profile across the expansion, see figures 7c and 7b, respectively. As a consequence, the angle encompassed by the rarefaction fan is larger than that observed for pure fluid MDM. The opposite situation is found in case 6d and the fan is narrower than its pure fluid counterpart.

From table 1 and figure 4, for small concentrations of MDM ( $x_{\text{MDM}} < 0.15$ ),  $\Gamma$  assumes negative values in the vapour phase and nonclassical behaviour is admissible. This is the case of the flow of mixture MDM(0.05)/MD<sub>6</sub>M(0.95) in figure 6e, where the expansion occurs through a nonclassical composite wave made of a continuous fan that is terminated by a nonclassical rarefaction shock wave, with close-to-sonic downstream state. The expansion is depicted in the thermodynamic plane in figure 5b, which displays the pre- and post-expansion states A and B in the reduced  $P$ - $v$  plane. While for the case of the pure fluid MD<sub>6</sub>M a single rarefaction shock wave connects the two states, in the case of the mixture MDM(0.05)/MD<sub>6</sub>M(0.95), an initial isentropic expansion is observed from state A to state A', which lies on the double sonic line. Then, a rarefaction shock wave expands the fluid from A' to B.

Results are summarized in table 4, which displays the downstream Mach number  $M$  and the variations of pressure  $P$ , the temperature  $T$ , the density  $\rho$  and the velocity  $u$  across the waves for all the considered different mixture compositions. The entropy difference across composite waves and the RSW is very small, due to both the relatively small pressure difference across the shock and the small value of  $\Gamma$ . Indeed, Landau & Lifshitz (1959) showed that a Taylor-series expansion of the Rankine-Hugoniot jump conditions delivers the following relation

$$\Delta s \simeq -\frac{\Gamma_A}{6} \frac{c_A^2}{T_A} \left[ \frac{\Delta v}{v_A} \right]^3 + o\left( \left[ \frac{\Delta v}{v_A} \right]^4 \right),$$

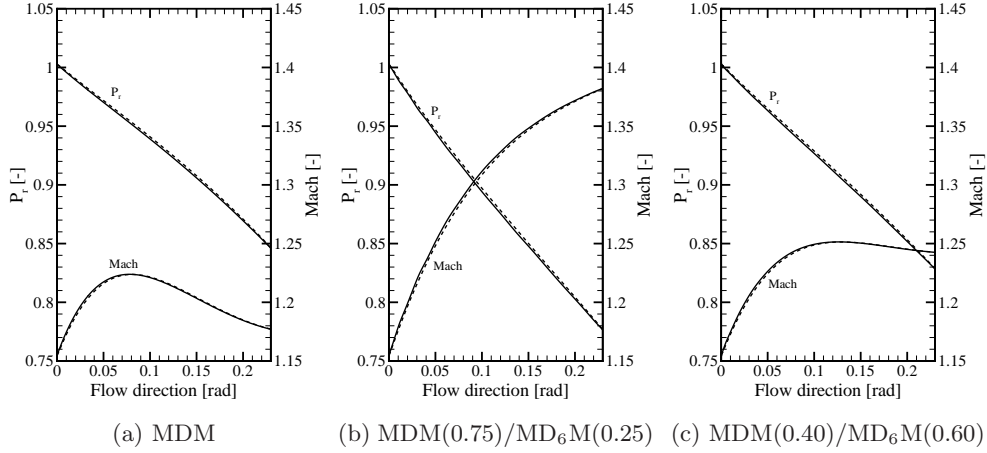


Figure 8: Comparison between the numerical integration ( - - ) of the Prandtl–Meyer ordinary differential equation (3.3) and numerical simulation (—).

where  $\Delta(\cdot) = (\cdot)_B - (\cdot)_A$ , which is valid for weak shock waves. In the present study, the largest entropy difference was computed by solving the non-linear Rankine-Hugoniot jump conditions for the RSW in MD<sub>6</sub>M and it is as small as  $\frac{\Delta s}{s_A} \sim 5 \times 10^{-6}$ .

To conclude, figure 8 reports the comparison of the numerical integration of the Prandtl–Meyer ordinary differential equation (3.3) and the numerical simulations for the three classical expansions of pure fluid MDM and of the mixtures MDM(0.75)/MD<sub>6</sub>M(0.25) and MDM(0.40)/MD<sub>6</sub>M(0.60). The very good agreement obtained by these two different approaches increases the authors’ confidence on the correctness of the presented results. Furthermore, the values of the upstream and downstream entropy were compared for the three isentropic expansions, for which the exact results is  $\frac{\Delta s}{s_A} \equiv 0$  since  $s_A \equiv s_B$ . Small relative differences of about  $10^{-6}$  confirmed that effects of numerical dissipation were negligible.

#### 4. Conclusions

Nonclassical gasdynamic phenomena in dense vapours of organic mixtures have been investigated for the first time. In particular, the effect of non-ideal mixing on the thermodynamic properties relevant to the fluid dynamics was studied.

Predictive equations of state have been used to compute the thermodynamic properties of the mixture, most notably the fundamental derivative of gasdynamicis  $\Gamma$ , for mixtures of siloxanes, perfluorocarbons, and siloxanes-perfluorocarbons. Some of the exemplary mixtures display thermodynamic regions of negative nonlinearity for certain compositions. The dependence of the minimum value of  $\Gamma$  in the vapour phase from the molar composition has been analysed in the paradigmatic case of mixtures of linear siloxanes. It is found that  $\Gamma_{\min}$  is always greater than the value of  $\Gamma_{\min}$  of the most complex molecule in the mixture. In addition the value  $\Gamma_{\min}$  of a pure linear siloxane whose molecular weight is intermediate with respect to that of the mixture constituents, is always lower than that of the mixture featuring the same molecular weight or complexity.

Preliminary simulations of a supersonic flow of a dense vapour expanding over a corner are presented. The dense vapour is a binary mixture of linear siloxanes MDM/MD<sub>6</sub>M,

whereby for each simulation the upstream conditions are kept similar, while the molar composition is varied from  $x_{\text{MDM}} = 0$  to  $x_{\text{MDM}} = 1$ . The results show how the flow field changes from the classical expansion fan to a rarefaction shock wave, when the composition is MDM(0.05)/MD<sub>6</sub>M(0.95). For MDM(0.15)/MD<sub>6</sub>M(0.85) a mixed rarefaction shock/fan is predicted. Thermal decomposition of the fluid and critical point effects are to be carefully assessed before selecting the substance for experiments. However, it is remarkable that, similarly to previous studies on non-classical flows, the same gasdynamics behaviour is expected for all considered fluids.

We conclude that for the considered mixtures, mixing compounds of the same fluid family does not enhance non-classical gasdynamic phenomena. Given the variety and complexity of molecular interactions among different molecules, the possibility that the opposite effect occurs for different mixture compositions should not be ruled out. Limitations with respect to accuracy and predictive character of currently available thermodynamic models for mixtures make the analysis of the possibly large variety of mixtures difficult. In addition, these limitations must be considered also with respect to the results of this study.

Future work will be devoted to the improvement of thermodynamic models suitable for complex organic compounds, possibly also by means of property measurements. Indeed, the main obstacle to such investigation is the lack of experimental thermodynamic data of mixtures of complex organic compounds, or of predictive and accurate thermodynamic models, valid close to the vapour-liquid critical point.

Attention will be dedicated to highly non-ideal mixtures in an attempt to understand if an enhancement of non-classical gasdynamic effects can be achieved by mixing two or more different organic fluids. This possibility—together with thermal stability—would have a large impact on experiments aimed at generating and measuring non-classical gasdynamic phenomena. Siloxane mixtures will also be tested in the experimental facility for generating and measuring rarefaction shock wave at the Delft University of Technology.

This research is supported by the Dutch Technology Foundation STW, and the Technology Program of the Ministry of Economic Affairs, project DSF 11143. The authors acknowledge the contribution of their colleague and friend T.P. van der Stelt for development of the mixture thermodynamic models.

## Appendix A. iPRSV-WS Thermodynamic model

The thermodynamic model adopted for the multi-component fluids is briefly described here. The volumetric equation of state (EoS) is provided by the so-called improved Stryjek-Vera Peng-Robinson (iPRSV) model complemented by a usual polynomial expression for the isobaric ideal-gas specific heat, see [van der Stelt \*et al.\* \(2012\)](#), and by the [Wong & Sandler \(1992a\)](#) mixing rules.

[Stryjek & Vera \(1986\)](#), see also [Proust & Vera \(1989\)](#), proposed to use the Peng Robinson ([Peng & Robinson 1976](#)) cubic EoS, with the Soave ([Soave 1972](#))  $\alpha$ -function, but with a different temperature and acentric factor dependence in order to improve the correlation of vapor pressures for a wide variety of fluids. Notably, the proposed functional form for  $\alpha$  results in the Stryjek-Vera Peng-Robinson (PRSV) EoS featuring a discontinuity in all the properties at the absolute critical temperature,  $T_c$ , for water and alcohols, and at temperature  $T = 0.7 \cdot T_c$  for all the other fluids. Recently, [van der Stelt \*et al.\* \(2012\)](#) proposed a modification of the PRSV EoS aimed at eliminating the discontinuity in the prediction of thermodynamic properties.



The iPRSV EoS is similar to the cubic form proposed by Peng & Robinson (1976),

$$P = \frac{RT}{v-b} - \frac{a}{v^2 + 2bv - b^2}, \quad (\text{A } 1)$$

where,

$$a = (0.457235 R^2 T_c^2 / P_c) \alpha, \quad b = 0.077796 RT_c / P_c, \quad \alpha = \left[ 1 + \kappa \left( 1 - \sqrt{T_r} \right) \right]^2.$$

$R$  is the universal gas constant,  $a$  is the attractive term,  $b$  is the co-volume parameter,  $P$  and  $v$  are the pressure and the specific volume, respectively. The subscript  $c$  indicates properties at the vapour-liquid critical point. The parameter  $\kappa$  depends on the temperature as follows

$$\kappa = \kappa_0 + \kappa_1 \left( 1 + \sqrt{T_r} \right) (0.7 - T_r), \quad (\text{A } 2)$$

with

$$\kappa_0 = 0.378893 + 1.4897153\omega - 0.17131848\omega^2 + 0.0196554\omega^3, \quad (\text{A } 3)$$

where  $\omega$  is the acentric factor. The empirical parameter  $\kappa_1$  in eq. (A 2) is a pure-component parameter fitted in order to obtain accurate predictions of saturated properties. From low temperatures up to reduced temperatures of  $T_r = 0.7$ , Stryjek and Vera recommend using values for  $\kappa_1$  tabulated in their papers (Stryjek & Vera 1986; Proust & Vera 1989). Alternatively,  $\kappa_1$  can also be obtained by regressing experimental data. According to Stryjek and Vera, for water and alcohols the tabulated values can be applied up to the critical point. For other compounds, slightly better results are obtained with  $\kappa_1 = 0$  for  $0.7 < T_r < 1$ . For super critical temperatures ( $T_r \geq 1$ ) they recommend  $\kappa_1 = 0$ , because there would be no advantage in using eq. (A 2) in this region. The  $\kappa$ -function therefore introduces a discontinuity in  $\alpha(T)$  either at  $T_r = 0.7$  or at  $T_r = 1$ , and in thermodynamic properties dependent upon and derivatives thereof. The iPRSV EoS is obtained by modifying the equation for the calculation of the  $\kappa$ -value, such that it is continuous with the temperature, but by keeping the same parameters  $\kappa_0$  and  $\kappa_1$  in the functional form, and in such a way that the same values can be used. This is a notable advantage, because a large amount of data for these parameters that have been obtained so far can still be used. The  $\kappa$ -function in the iPRSV thermodynamic model is therefore

$$\kappa = \kappa_0 + \kappa_1 \left\{ \sqrt{[A - D(T_r + B)]^2 + E} + A - D(T_r + B) \right\} \sqrt{T_r + C}, \quad (\text{A } 4)$$

where the value of the coefficients are  $A = 1.1$ ,  $B = 0.25$ ,  $C = 0.2$ ,  $D = 1.2$  and  $E = 0.01$ . The accuracy of the iPRSV thermodynamic model is similar or better than that of the model from which is derived. The derivatives of  $\kappa$  with respect to the temperature, that are required for the implementation of a complete thermodynamic model into a computer program, are given by van der Stelt *et al.* (2012) together with a thorough discussion on the limits of the thermodynamic model.

Wong & Sandler (1992a) developed a set of mixing rules which satisfy the theoretically correct quadratic composition dependence of the second virial coefficient. The mixing rule is derived by equating the excess Helmholtz energy  $A^E$  of an activity coefficient model describing molecular interaction in the liquid phase to that obtained from the EoS at the so-called infinite-pressure state, namely, in the limit of a specific volume approaching the co-volume. The mixing rule contains one additional binary interaction parameter  $k_{ij}$  in the cross second virial coefficient, see Eq. A 7. The binary interaction parameter can be determined by various approaches, see e.g. Coutsikos *et al.* (1995a). The Wong-Sandler

mixing rule (WSMR) is used extensively in conjunction with the PRSV EoS. For the activity coefficient model, a so-called “solely energetic” model is usually preferred (i.e., a model which does not have an explicit free-volume term). As it is common practice for the PRSV EoS, the NRTL model introduced by [Renon & Prausnitz \(1968\)](#) is used here to compute the activity coefficient, see also [Ghosh & Taraphdar \(1998\)](#).

According to the WSMR, the  $a$  and  $b$  coefficients in (A 1) are substituted by

$$a_M = RTDb_M, \quad \text{and} \quad b_M = \frac{Q}{1-D}, \quad (\text{A } 5)$$

respectively, where

$$D = \frac{A_\infty^E}{C_{\text{EoS}}} + \sum_{i=1}^{\text{NC}} \frac{x_i a_i}{RTb_i}, \quad Q = \sum_{i=1}^{\text{NC}} \sum_{j=1}^{\text{NC}} x_i x_j \left( b - \frac{a}{RT} \right)_{ij}.$$

The parameter  $C_{\text{EoS}}$  depends upon the equation of state. For the PRSV EOS, it reads

$$C_{\text{EoS}} = \frac{\sqrt{2}}{2} \ln(\sqrt{2} - 1) \approx -0.62323. \quad (\text{A } 6)$$

The following combining rule has been used

$$\left( b - \frac{a}{RT} \right)_{ij} = \frac{b_i + b_j - a_i + a_j}{2RT} (1 - k_{ij}). \quad (\text{A } 7)$$

where  $a$  and  $b$  are the energy and the co-volume parameter. The subscript M refers to mixture properties while  $i$  and  $j$  refer to the components in the mixture. NC is the number of components.

From the pressure EoS, a complete thermodynamic model can be finally obtained by specifying the relation between the temperature and the specific heat at constant pressure  $c_P$  in the dilute gas limit, see e.g. [Callen \(1985\)](#). In the present study, the following functional form of  $c_P$

$$\psi(T) = \lim_{v \rightarrow \infty} c_P(T, v) = C_0 + C_1 T + C_2 T^2 + C_3 T^3 \quad (\text{A } 8)$$

with  $C_0, C_1, C_2$  and  $C_3$  constants. The values of the parameters  $C_0, C_1, C_2$  and  $C_3$  are given by [van der Stelt \*et al.\* \(2012\)](#) for the fluids of interest here. From the  $c_P$  definition (A 8) and the pressure EoS (A 1) a complete thermodynamic model can be obtained. For example, from the reciprocity relation, one immediately computes the energy EoS as

$$e(T, v) = \phi(T) + \int_{v_0}^v \left[ T \frac{\partial P(T, \nu)}{\partial \nu} - P \right] d\nu \quad (\text{A } 9)$$

where, from the Meyer’s law of ideal gas,  $\phi(T) = \psi(R) - R = \lim_{v \rightarrow \infty} c_v(T, v)$  is the specific heat at constant volume in the dilute gas limit. All thermodynamic variables can be computed from the two pressure and energy EoS (A 1) and (A 9), respectively, as detailed, e.g., by [Colonna & Silva \(2003b\)](#).

## REFERENCES

- ABBOTT, M. M. 1973 Cubic Equations of State. *AICHE J.* **19**, 596–601.
- ALDO, A. & ARGROW, B. 1995 Dense gas flow in minimum length nozzles. *J. Fluid Eng.-T. ASME* **117** (2), 270–276.
- ANGELINO, G. & COLONNA, P. 1998 Multicomponent working fluids for organic Rankine cycles (ORCs). *Energy* **23** (6), 449–463.
- ANGELINO, G. & COLONNA, P. 2000 Air cooled siloxane bottoming cycle for molten carbonate fuel cells. In *Fuel Cell Seminar*, pp. 667–670.

- ANGELINO, G. & INVERNIZZI, C. 1993 Cyclic methylsiloxanes as working fluids for space power cycles. *J. Sol. Energy. - Trans. ASME* **115** (3), 130–137, cited By (since 1996) 23.
- ARGROW, B. M. 1996 Computational analysis of dense gas shock tube flow. *Shock Waves* **6**, 241–248.
- ARMENIO, A. 2009 Siloxane/perfluorocarbon mixtures as working fluid for organic Rankine cycle turbogenerators. Master's thesis, Politecnico di Milano - Delft University of Technology, ET-2365.
- BETHE, H. A. 1942 The theory of shock waves for an arbitrary equation of state. Technical report 545. Office Sci. Res. & Dev.
- BORISOV, A. A., BORISOV, A. L. AND KUTATELADZE, S. S. & NAKORYAKOV, V. E. 1983 Rarefaction shock waves near the critic liquid-vapour point. *J. Fluid Mech.* **126**, 59–73.
- BROWN, B. & ARGROW, B. 1997 Two-dimensional shock tube flow for dense gases. *J. Fluid Mech.* **349**, 95–115.
- BROWN, B. & ARGROW, B. 1998 Nonclassical dense gas flows for simple geometries. *AIAA J.* **36** (10), 1842–1847.
- BROWN, B. & ARGROW, B. 2000 Application of Bethe–Zel'dovich–Thompson fluids in organic Rankine cycle engines. *J. Propul. Power* **16** (6), 1118–1124.
- BYMASTER, A., EMBORSKY, C., DOMINIK, A. & CHAPMAN, W. 2008 Renormalization-group corrections to a perturbed-chain statistical associating fluid theory for pure fluids near to and far from the critical region. *Ind. Eng. Chem. Res.* **47** (16), 6264–6274.
- CALLEN, H. B. 1985 *Thermodynamics and an introduction to thermostatistics*, 2nd edn. Wiley.
- CHANDRASEKAR, D. & PRASAD, P. 1991 Transonic flow of a fluid with positive and negative nonlinearity through a nozzle. *Phys. Fluids A* **3** (3), 427–438.
- CHEN, H., GOSWAMI, D. Y., RAHMAN, M. M. & STEFANAKOS, E. K. 2011 A supercritical Rankine cycle using zeotropic mixture working fluids for the conversion of low-grade heat into power. *Energy* **36** (1), 549–555.
- CINNELLA, P. 2008 Transonic flows of dense gases over finite wings. *Phys. Fluids* **20** (4).
- CINNELLA, P. & CONGEDO, P. M. 2007 Inviscid and viscous aerodynamics of dense gases. *J. Fluid Mech.* **580**, 179–217.
- CINNELLA, P. & CONGEDO, P. M. 2008 Optimal airfoil shapes for viscous transonic flows of Bethe–Zel'dovich–Thompson fluids. *Comput. & Fluids* **37**, 250–264.
- COLONNA, P. 1996 Fluidi di lavoro multi componenti per cicli termodinamici di potenza (multicomponent working fluids for power cycles). PhD thesis, Politecnico di Milano.
- COLONNA, P. & GUARDONE, A. 2006 Molecular interpretation of nonclassical gas dynamics of dense vapors under the van der Waals model. *Phys. Fluids* **18** (5).
- COLONNA, P., GUARDONE, A. & NANNAN, N. R. 2007 Siloxanes: A new class of candidate Bethe–Zel'dovich–Thompson fluids. *Phys. Fluids* **19** (8).
- COLONNA, P., GUARDONE, A., NANNAN, N. R. & ZAMFIRESCU, C. 2008a Design of the dense gas flexible asymmetric shock tube. *J. Fluid Eng.-T. ASME* **130** (3), 0345011–0345016.
- COLONNA, P., NANNAN, N. R. & GUARDONE, A. 2008b Multiparameter equations of state for siloxanes:  $[(\text{CH}_3)_3\text{-Si-O}_{1/2}]_2\text{-[O-Si-(CH}_3)_2]_{i=1,\dots,3}$  and  $[\text{O-Si-(CH}_3)_2]_6$ . *Fluid Phase Equilib* **263** (2), 115–130.
- COLONNA, P., NANNAN, N. R., GUARDONE, A. & LEMMON, E. W. 2006 Multiparameter equations of state for selected siloxanes. *Fluid Phase Equilib.* **244**, 193–211.
- COLONNA, P., NANNAN, N. R., GUARDONE, A. & VAN DER STELT, T. P. 2009 On the computation of the fundamental derivative of gas dynamics using equations of state. *Fluid Phase Equilib.* **286** (1), 43–54.
- COLONNA, P. & SILVA, P. 2003a Dense gas thermodynamic properties of single and multicomponent fluids for fluid dynamics simulations. *J. Fluid Eng.-T. ASME* **125** (3), 414–427.
- COLONNA, P. & SILVA, P. 2003b Dense gas thermodynamic properties of single and multicomponent fluids for fluid dynamics simulations. *ASME J. Fluids Eng.* **125**, 414–427.
- COLONNA, P., VAN DER STELT, T. P. & GUARDONE, A. 2012 FluidProp (Version 3.0): A program for the estimation of thermophysical properties of fluids. <http://www.fluidprop.com/>, a program since 2004.
- CONGEDO, P., COLONNA, P., CORRE, C., WITTEVEEN, J. & IACCARINO, G. 2012 Backward uncertainty propagation method in flow problems: application to the prediction of rarefaction shock waves. *Comput Method Appl M* **213–216**, 314–326.

- COUTSIKOS, P., KALOSPIROS, N. & TASSIOS, D. 1995a Capabilities and limitations of the Wong-Sandler mixing rules. *Fluid Phase Equilibria* **108** (1-2), 59–78.
- COUTSIKOS, P. *et al.* 1995b Capabilities and limitations of the Wong-Sandler Mixing Rules. *Fluid Phase Equilib.* **108**, 59–78.
- CRAMER, M. & KLUWICK, A. 1984 On the propagation of waves exhibiting both positive and negative nonlinearity. *J. Fluid Mech.* **142**, 9–37.
- CRAMER, M. S. 1989 Negative nonlinearity in selected fluorocarbons. *Phys. Fluids* **1** (11), 1894–1897.
- CRAMER, M. S. 1991 Nonclassical dynamics of classical gases. In *Nonlinear Waves in Real Fluids* (ed. A. Kluwick), pp. 91–145. Springer-Verlag.
- CRAMER, M. S. & BEST, L. M. 1991 Steady, isentropic flows of dense gases. *Phys. Fluids A* **3** (1), 219–226.
- CRAMER, M. S. & CRICKENBERGER, A. B. 1991 The dissipative structure of shock waves in dense gases. *J. Fluid Mech.* **223**, 325–355.
- CRAMER, M. S. & SEN, R. 1986 Shock formation in fluids having embedded regions of negative nonlinearity. *Phys. Fluids* **29**, 2181–2191.
- CRAMER, M. S. & SEN, R. 1987 Exact solutions for sonic shocks in van der waals gas. *Phys. Fluids* **30** (2), 377–385.
- CRAMER, M. S. & SEN, R. 1990 Mixed nonlinearity and double shocks in superfluid helium. *J. Fluid Mech.* **221**, 233–261.
- CRAMER, M. S., TARKENTON, L. M. & TARKENTON, G. M. 1992 Critical Mach number estimates for dense gases. *Phys. Fluids A* **4** (8), 1840–1847.
- DVORNIC, P. R. 2004 *Silicon Compounds: Silanes and Silicones*, chap. High Temperature Stability of Polysiloxanes, pp. 419–432. Gelest Inc.
- FERGASON, S. H. 2001 Dense gas shock tube: design and analysis. Ph.d. thesis, University of Colorado, Boulder.
- FERGASON, S. H., GUARDONE, A. & ARGROW, B. M. 2003 Construction and validation of a dense gas shock tube. *J. Thermophys. Heat Tr.* **17** (3), 326–333.
- FERGASON, S. H., HO, T. L., ARGROW, B. M. & EMANUEL, G. 2001 Theory for producing a single-phase rarefaction shock wave in a shock tube. *J. Fluid Mech.* **445**, 37–54.
- GHOSH, P. & TARAPHDAR, T. 1998 Prediction of vapor-liquid equilibria of binary systems using PRSV equation of state and Wong-Sandler mixing rules. *Chemical Engineering Journal* **70** (1), 15–24.
- GROSS, J. & SADOWSKI, G. 2001 Perturbed-chain SAFT: An equation of state based on a perturbation theory for chain molecules. *Ind. Eng. Chem. Res.* **40** (4), 1244–1260.
- GUARDONE, A. 2007 Three-dimensional shock tube flows of dense gases. *J. Fluid Mech.* **583**, 423–442.
- GUARDONE, A., ZAMFIRESCU, C. & COLONNA, P. 2010 Maximum intensity of rarefaction shock waves for dense gases. *J. Fluid Mech.* **642** (1), 127–146.
- GULEN, S. C., THOMPSON, P. A. & CHO, H. A. 1989 Rarefaction and liquefaction shock waves in regular and retrograde fluids with near-critical end states. In *Adiabatic waves in liquid-vapor systems*, pp. 281–290. Springer-Verlag.
- HAYES, W. 1960 The basic theory of gasdynamic discontinuities. In *Fundamentals of gasdynamics: High speed aerodynamics and jet propulsion* (ed. H. W. Emmons), , vol. 3, pp. 416–481. Princeton University Press.
- IVANOV, A. G. & NOVIKOV, S. A. 1961 Rarefaction shock waves in iron and steel. *Zh. Eksp. Teor. Fiz.* **40** (6), 1880–1882.
- KLUWICK, A. 2001 *Handbook of shockwaves*, , vol. 1, chap. 3.4 (Theory of shock waves. Rarefaction shocks.), pp. 339–411. Academic Press.
- KLUWICK, A. & MEYER, G. 2010 Shock regularization in dense gases by viscous-inviscid interactions. *Journal of Fluid Mechanics* **644**, 473–507.
- KUNZ, O., KLIMECK, R., WAGNER, W. & JAESCHKE, M. 2007 The GERG-2004 wide-range equation of state for natural gases and other mixtures. *Tech. Rep.*. GERG Technical Monograph 15, VDI-Verlag.
- KUTATELADZE, S. S., NAKORYAKOV, V. E. & BORISOV, A. A. 1987 Rarefaction waves in liquid and gas-liquid media. *Ann. Rev. Fluid Mech.* **19**, 577–600.

- LAI, N., WENDLAND, M. & FISCHER, J. 2009 Description of linear siloxanes with PC-SAFT equation. *Fluid Phase Equilib.* **283** (1-2), 22–30.
- LANDAU, L. D. & LIFSHITZ, E. M. 1959 *Course of theoretical physics, fluid mechanics*, , vol. 6. Pergamon Press, Oxford.
- LANG, W., ALMBAUER, R. & COLONNA, P. 2013 Assessment of waste heat recovery for a heavy-duty truck engine using an ORC turbogenerator. *Journal of Engineering for Gas Turbines and Power-Transactions of the ASME* **135** (4), 042313–1–10.
- MENIKOFF, R. & PLOHR, B. J. 1989 The Riemann problem for fluid flow of real material. *Rev. Mod. Phys.* **61** (1), 75–130.
- MONACO, J., CRAMER, M. & WATSON, L. 1997 Supersonic flows of dense gases in cascade configurations. *J. Fluid Mech.* **330**, 31–59.
- NANNAN, N. R., COLONNA, P., TRACY, C. M., ROWLEY, R. L. & HURLY, J. J. 2007 Ideal-gas heat capacities of dimethylsiloxanes from speed-of-sound measurements and ab initio calculations. *Fluid Phase Equilib.* **257** (1), 102–113.
- NANNAN, N. R., GUARDONE, A. & COLONNA, P. 2013 On the fundamental derivative of gas dynamics in the vapor-liquid critical region of single-component typical fluids. *Fluid Phase Equilib.* **337**, 259–273.
- NANNAN, R. N. & COLONNA, P. 2009 Improvement on multiparameter equations of state for dimethylsiloxanes by adopting more accurate ideal-gas isobaric heat capacities: Supplementary to P. Colonna, N. R. Nannan, A. Guardone, E. W. Lemmon, *Fluid Phase Equilib.* 244, 193 (2006). *Fluid Phase Equilib.* **280** (1–2), 151–152, short Communication.
- PECNIK, R., RINALDI, E. & COLONNA, P. 2012a Computational fluid dynamics of a radial compressor operating with supercritical CO<sub>2</sub>. *Journal of Engineering for Gas Turbines and Power-Transactions of the ASME* **134**, 122301.
- PECNIK, R., TERRAPON, V. E., HAM, F., IACCARINO, G. & PITSCH, H. 2012b Reynolds-Averaged Navier-Stokes Simulations of the Hyshot II Scramjet. *AIAA J.* **50** (8), 1717–1732.
- PENG, D. Y. & ROBINSON, D. B. 1976 A new two-constant equation of state. *Ind. Eng. Chem. Fundam.* **15** (1), 59–64.
- PROUST, P. & VERA, J. H. 1989 PRSV: The Stryjek-Vera modification of the Peng-Robinson equation of state. parameters for other pure compounds of industrial interest. *The Canadian Journal of Chemical Engineering* **67** (1), 170–173.
- RENON, H. & PRAUSNITZ, J. M. 1968 Local compositions in thermodynamic excess functions for liquid mixtures. *AIChE Journal* **14** (1), 135–144.
- SANDLER, S. I. 1989 *Chemical and Engineering Thermodynamics*, 2nd edn. New York: John Wiley and Sons.
- SANDLER, S. I. 1993 *Models for Thermodynamic and Phase Equilibria Calculations*. CRC Press.
- SCHNERR, G. & MOLOKOV, S. 1994 Exact solutions for transonic flows of dense gases in two-dimensional and axisymmetric nozzles. *Phys. Fluids* **6** (10), 3465–3472.
- SCHNERR, G. & MOLOKOV, S. 1995 Nonclassical effects in two-dimensional transonic flows. *Phys. Fluids* **7** (11), 2867–2875.
- SCHNERR, G. H. & LEIDNER, P. 1993a Numerical investigation of axial cascades for dense gases. In *PICAST1–Pacific International Conference on Aerospace Science Technology* (ed. E. L. Chin), , vol. 2, pp. 818–825. National Cheng Kung University, Taiwan, Republic of China.
- SCHNERR, G. H. & LEIDNER, P. 1993b Two-dimensional nozzle flow of dense gases. In *Fluids Engineering Conference*. Washington, DC.
- SOAVE, G. 1972 Equilibrium constants from a modified Redlich-Kwong equation of state. *Chem. Eng. Sci.* **27**, 1197–1203.
- STRYJEK, R. & VERA, J. H. 1986 PRSV: An improved Peng–Robinson equation of state for pure compounds and mixtures. *Canadian Journal of Chemical Engineering* **64** (2), 323–333.
- THOMPSON, P. A. 1971 A fundamental derivative in gasdynamics. *Phys. Fluids* **14** (9), 1843–1849.
- THOMPSON, P. A. 1988 *Compressible Fluid Dynamics*. McGraw-Hill.
- THOMPSON, P. A. 1991 Liquid-vapor adiabatic phase changes and related phenomena. In *Non-linear Waves in Real Fluids* (ed. A. Kluwick), pp. 147–213. New York, NY: Springer-Verlag.
- THOMPSON, P. A., CAROFANO, G. A. & KIM, Y. G. 1986 Shock waves and phase changes in a large heat capacity fluid emerging from a tube. *J. Fluid Mech.* **166**, 57–96.
- THOMPSON, P. A. & LAMBRAKIS, K. C. 1973 Negative shock waves. *J. Fluid Mech.* **60**, 187–208.

- THOMPSON, P. A. & LOUTREL, W. F. 1973 Opening time of brittle shock-tube diaphragms for dense fluids. *Rev. Sci. Instrum.* **44** (9), 1436–1437.
- TRAPP, C. & COLONNA, P. 2013 Efficiency improvement in pre-combustion CO<sub>2</sub> removal units with a waste-heat recovery ORC power plant. *Journal of Engineering for Gas Turbines and Power-Transactions of the ASME* **135** (4), 042311–1–12.
- UUSITALO, A., TURUNEN-SAARESTI, T., HONKATUKIA, J., COLONNA, P. & LARJOLA, J. 2013 Siloxanes as working fluids for a mini-ORC systems based on high-speed turbogenerator technology. *Journal of Engineering for Gas Turbines and Power-Transactions of the ASME* **135** (4), 042305–1–9.
- VAN DER STELT, T. P., NANNAN, N. R. & COLONNA, P. 2012 The iPRSV equation of state. *Fluid Phase Equilib.* **330**, 24–35.
- VAN DER WAALS, J. D. 1988 *On the continuity of the gaseous and liquid states*, , vol. XIV. North-Holland, reprinted.
- WEYL, H. 1949 Shock waves in arbitrary fluids. *Comm. Pure Appl. Math.* **2**, 102–122.
- WONG, D. S. H. & SANDLER, S. I. 1992*a* A theoretically correct mixing rule for cubic equations of state. *AIChE J.* **38**, 671–680.
- WONG, D. S. H. & SANDLER, S. I. 1992*b* Theoretically correct mixing rule for cubic equations of state. *AIChE J.* **38** (5), 671–680.
- ZAMFIRESCU, C., GUARDONE, A. & COLONNA, P. 2008 Admissibility region for rarefaction shock waves in dense gases. *J. Fluid Mech.* **599**, 363–381.
- ZEL'DOVICH, Y. 1946 On the possibility of rarefaction shock waves. *Zh. Eksp. Teor. Fiz.* **4**, 363–364.